

Identifying the Lateral Component of Drainage Flux in Hill Slopes

D. Rassam^a and M. Littleboy^b

^aDepartment of Natural Resource and Mines, Brisbane QLD, Australia.

^bDepartment of Land and Water Conservation, NSW, Australia.

Abstract: Accurate prediction of recharge under various land uses is a crucial component for modelling the risk of dryland salinity. One-dimensional water balance models can be readily applied but assume all excess soil water drains vertically to the watertable. To improve the prediction of recharge from 1D models, a simple algorithm to partition excess soil water into lateral and vertical pathways has been determined from more complex soil water modelling. HYDRUS-2D was adopted to partition the lateral and vertical components of drainage flux in hill slopes of varying steepness with a duplex soil system whereby a coarse layer overlays a fine layer. Results of the numerical simulations have shown that the slope angle (θ) and the hydraulic conductivity ratio (K_r) of the two draining soils in the duplex system dictate the partitioning factor of drainage flux R_h (defined as cumulative lateral flow at end of drainage / initial water volume store in soil block under consideration). In an extreme case of a sand-clay duplex system sloping at 15° , 93% of the moisture in the soil profile drains laterally. We propose a mathematical function that describes the 3-dimensional surface plotted in the " R_h - K_r - θ " space. The second partial derivative of the proposed function ($\partial^2 R_h / \partial \theta \partial K_r$) revealed that R_h is most sensitive to K_r values ranging from 1 to 150 and θ of up to 15° .

Keywords: *Perched water table; Drainage flux; ; Modelling; Salinity*

1. INTRODUCTION

Salinity models are critical to guide investment decisions, catchment planning activities and future salt loads trends analyses under State, Murray-Darling Basin and National Strategies. In eastern Australia, salinity management planning is underpinned by the concept of a future salt target. Intervention strategies (e.g., land use changes) are designed and implemented so that a catchment may achieve its target. There is an urgent need to develop a predictive "cause and effect" capability so that the contributions of different intervention strategies on achieving catchment targets can be quantified. Therefore, to support these strategies, hydrological and salt balance models must reflect the land use changes within a catchment on salt export from a catchment. A current focus for salinity investment is to target areas in the landscape where tree planting and other land use change will reduce salt export from a catchment. To enable this output, salinity modelling incorporates information on where salt is stored in the landscape and how much there is, and identifies how much salt is mobilised by surface runoff, subsurface flow or groundwater discharge; and

what the impacts of land use change on hydrology and salt export are at property, catchment, and river basin scales

One aspect of such an integrated suite of models is the capability to predict recharge to groundwater under various land use and land management scenarios to identify areas where a land use change (e.g. tree planting) will have the highest impact on recharge.

Previous studies throughout Australia have highlighted inadequacies in applying one-dimensional unsaturated zone water balance models to estimate recharge. These models estimate vertical deep drainage but ignore lateral movement of water. Estimated deep drainage from unsaturated zone models is often greater than recharge estimated from the calibration of groundwater models (Stauffacher et al., 2000).

The advantage of applying one-dimensional water balance models to estimate deep drainage is the relative ease of parameterisation. Many two-dimensional water balance models are available but the increased data requirements for these types of models, can limit their usefulness in producing maps of recharge on a regional or statewide basis.

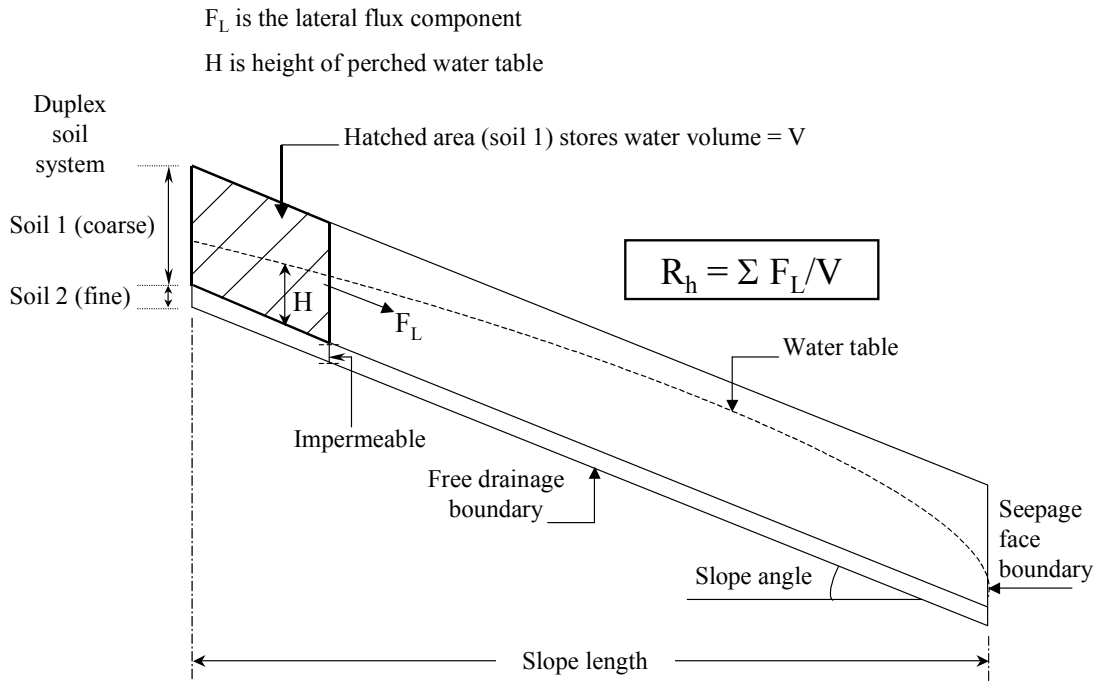


Figure 1: Conceptual model, boundary conditions, and definition of relevant terms

The formation and drainage of perched water tables have been investigated by many researchers (Wooding, 1966; Chapman and Dressler, 1984). However, they don't account for water passing through the low-permeability layer. In this study, we use HYDRUS-2D (Simunek et al., 1999) to estimate the lateral component of flux and present a simple mathematical relationship that describes it; this relationship can then readily be used in simpler 1-D models. In this way, we capture the complexity of processes driving what can be substantial lateral water movement into a simple modelling approach that can be readily applied using existing data.

2. MODELLING HILL SLOPE HYDROLOGY

2.1. Conceptual Model

The problem is conceptualised as shown in Figure 1. The slope length extends between the left uppermost side on the slope, represented by a no-flow boundary, and the right lowermost side on the slope, represented by a seepage face. The lower boundary is assumed to be freely draining, that is, gravity unit-gradient flow conditions prevail. A duplex soil system whereby a coarse textured soil overlays a fine textured soil is

always assumed; this configuration promotes a perched water table.

The soil profile is initially saturated. The pressure head at the sloping surface is equal to zero and hydrostatic equilibrium is assumed. The profile is allowed to drain; drainage flux comprises a lateral component F_L and a downward component F_v ; the latter represents recharge to the water table.

Referring to Figure 1, the water mass balance of the hatched area is considered. Note that the trapezoidal shape has equal sides so that F_v and F_L are integrated over equal distances. The volume fraction that drains laterally is defined as follows:

$$R_h = \frac{\sum F_L}{V} \quad (1)$$

where R_h is the lateral drainage fraction, $\sum F_L$ is the cumulative flow drained laterally (flux integrated in space and time), and V is to the total water volume stored in the soil block under consideration prior to drainage.

2.2. Pilot simulations

A number of pilot simulations were conducted in order to gain an insight into the effects of slope angle, soil type, and slope length. We model a slope 20-m wide and 5-m high.

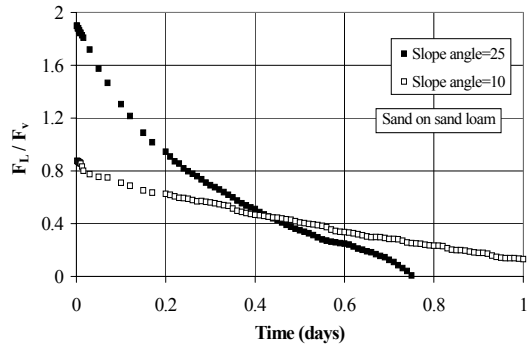


Figure 2. Flux ratios versus drainage time for ‘sand on sand loam’

Two contrasting duplex soil systems are used, namely, ‘sand on sand loam’, and ‘sand on clay loam’. The hydraulic conductivity ratio is defined as: $K_r = K_{\text{top layer}} / K_{\text{underlying layer}}$. Table 1 shows that the respective hydraulic conductivity ratios are 6.7 and 114. Drainage was simulated in two landscapes sloping at 10° and 25°. Referring to Figures 2 and 3, the following comments are made:

Table 1: K_r for various soil systems

Duplex soil system	K_r
Loam on clay	5.2
Sand on sand loam	6.7
Sand loam on clay	22
Sand on loam	28.5
Loamy sand on clay loam	58
Loamy sand on clay	70
Sand on clay loam	114
Sand on clay	148

- It is apparent that K_r has a significant effect on flux ratios. Hence for the duplex soil systems under consideration in this paper, K_r is always ≥ 1 ; a ratio of unity refers to a single layered system.
- For both soil systems, increasing the slope angle from 10° to 25° almost resulted in doubling the flux ratio, which indicates an increase in the lateral flux component.
- Figure 3 shows that for sand on clay loam case, the drainage curves flatten after 0.8 day, however, the flux ratio is still equal to 10. This is due to a low vertical flux component. Note how in the case of the steep 25°-slope, the flux ratio drops dramatically from 38 to 10 during the 0.8-day period. This is due to the fact that most of the water is drained laterally, which is attributable to a combination of high K_r and steep slope.

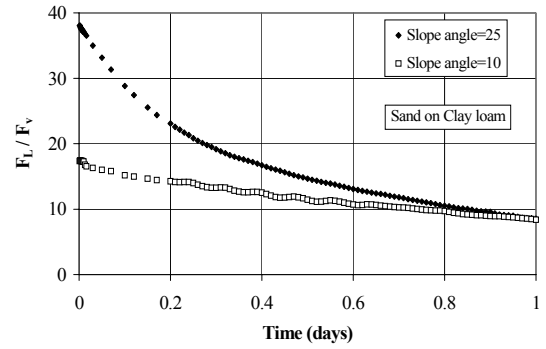


Figure 3. Flux ratios versus drainage time for ‘sand on clay loam’

Flux ratios are also plotted versus pressure head with the datum being the lower boundary of the profile (see ‘H’ in Figure 1). In Figure 4 we compare the 25°-slope data (where the lateral flux component is maximal) for ‘sand on sand-loam’ and ‘sand on clay-loam’. For both cases, as the pressure head exceeds a certain value (2.5 and 3.0 m), the flux ratio starts to increase in a non-linear manner. This is attributable to the effect of the seepage face. Ideally, the draining soil block under consideration should be far enough from the seepage face to avoid such non-linearity. Therefore, for the remaining simulations, we chose a domain where height/width ratio = 1:10. Hence, the soil block under consideration (hatched area in Figure 1) measures 2×2m, and slope length is 20 m. The 2-m high soil block means that the initial pressure head before drainage starts is equal to 2 m (since the initial water table is located at the surface). The duplex soil systems listed in Table 1 are investigated.

2.3. Simulation Results

The lateral drainage fraction R_h is basically a function of K_r and slope angle. Figure 5 shows the upper and lower bounds of R_h as a function of slope angle.

In a single layer soil system (of constant hydraulic

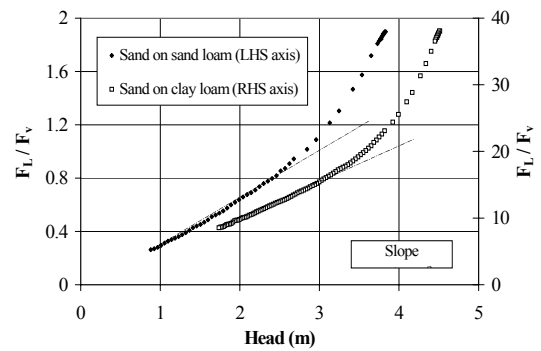


Figure 4. Flux ratios versus pressure head

conductivity $K_r=1$), where drainage is basically driven by gravity, R_h simply relates to the slope angle. For an infinite soil block, consider the extreme cases where the slope angle is either 0° (horizontal block) or 90° (vertical block). In the former case, $R_h=0$ meaning that there is no lateral drainage component since the seepage face is assumed to be distant. In the latter case, the soil block is vertical (note that for this case, our definition of horizontal flow becomes vertical), thus drainage is fully through the seepage face, i.e., $R_h=1$.

Intermediate cases will simply scale as the sine function of the slope angle, which is shown in Figure 5 (curve 1). This is the lower bound solution for any two-layered problem where a low-conductivity soil underlies a high-conductivity soil. Considering our simulations, curve (1) of Figure 5 represents the case where the hydraulic conductivity of the upper soil layer continues to drop until it becomes equal to that of the underlying layer (as in curves 4, 3, 2, then 1), that is, for the case shown in Figure 5, it becomes clay on clay ($K_r=1$), or simply a single clay layer.

Figure 5 shows that the upper bound solution for any soil system is $R_h=1$ when the slope angle approaches 90° . Intermediate values ($K_r=5, 21$, and 142) lie neatly between the upper and the lower bounds. Figure 5 (curve 4) shows that R_h becomes much higher even for a horizontal soil block (slope angle= 0 ; $R_h=0.6$). As $K_r \rightarrow \infty$, we approach the upper bound solution, which is $R_h=1$ regardless of the slope angle (curve 5, Figure 5). In reality, this condition represents a zero-flux boundary condition where the entire moisture is drained laterally via the seepage face.

Note that with the exception of curve 1 (which is basically a sine function), all R_h values for angles $>25^\circ$ were visually extrapolated. This was justifiable because the upper and lower bounds were clearly defined.

Figure 6 shows how R_h varies with K_r for three different slope angles. Note that regardless of individual soil type, it is K_r that always dictates R_h . We emphasize that the presented results are relevant to the imposed initial and boundary conditions. It was demonstrated in Figure 4 that the lateral component of flux varies directly with the initial water table height (i.e., depends on initial conditions).

3. MATHEMATICAL REPRESENTATION OF 3-D ENVELOPE DESCRIBING R_h

The simulation results are plotted in 3-dimensional space as shown in Figure 7. The

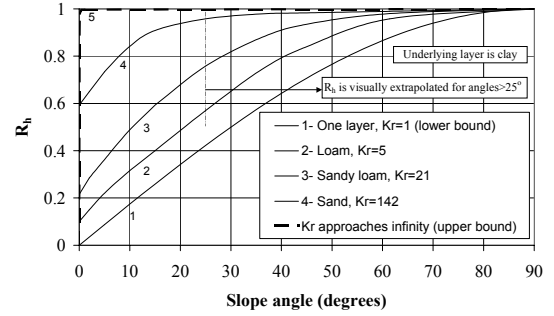


Figure 5. Upper and lower bound values for R_h

estimates of R_h obtained from HYDRUS-2D were input into the surface fitting software TableCurve-3D. Equation 2 was found to be suitable to describe the 3-D surface ($R_h - K_r - \theta$). Note that in Equation 2, θ is the slope angle, $a, b, c, d, e, f, g, h, i, j,$ and k are fitting parameters. The values for the fitting parameters are listed in Table 2. For high values of θ and K_r (especially when both are high), Equation (2) might result in R_h being slightly larger than 1, which is meaningless. Note that $0 \leq R_h \leq 1$.

Table 2: Fitting parameters for Equation 1.

a	0.04487
b	-0.11431
c	0.01979
d	-0.35073
e	-0.02060
f	0.01304
g	0.01010
h	0.04055
i	0.01415
j	0.01585
k	-0.01105

Predictions from Equation (2) were compared to the original estimates produced by HYDRUS-2D. The absolute error (percentage) was statistically analysed, the following results were obtained: mean error=2.77%; standard deviation of error=2.05%; maximum error=8.12%.

Analysing the second partial derivative of the function ($\partial^2 R_h / \partial K_r \partial \theta$) revealed that R_h is most sensitive to K_r values ranging from 1 to 150 and slope angles of up to 15° .

4. CONCLUSIONS

HYDRUS-2 was used to investigate the significance of lateral drainage in hill slopes.

Results have shown that the fraction of soil water draining laterally (R_h) correlates to slope angle and conductivity ratio (K_r) of the draining duplex soils. In an extreme case of a sand-clay duplex system ($K_r=148$) sloping at 15° , 93% of the water initially stored in the soil profile drains laterally. An empirical relationship is proposed to describe the variation of R_h with K_r and slope angle.

Analysing the second partial derivative of the proposed function ($\partial^2 R_h / \partial K_r \partial \theta$) revealed that R_h is most sensitive to K_r values ranging from 1 to 150 and θ of up to 15° .

$$R_h = \frac{a + c \ln(K_r) + e \ln(\theta) + g (\ln(K_r))^2 + i (\ln(\theta))^2 + k \ln(K_r) \ln(\theta)}{1 + b \ln(K_r) + d \ln(\theta) + f (\ln(K_r))^2 + h (\ln(\theta))^2 + j \ln(K_r) \ln(\theta)} \quad (2)$$

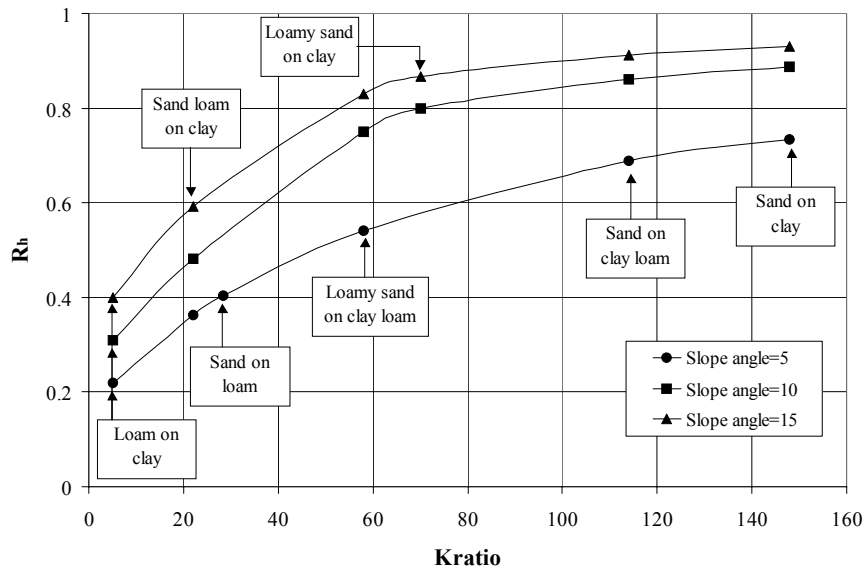


Figure 6: R_h for various soil systems

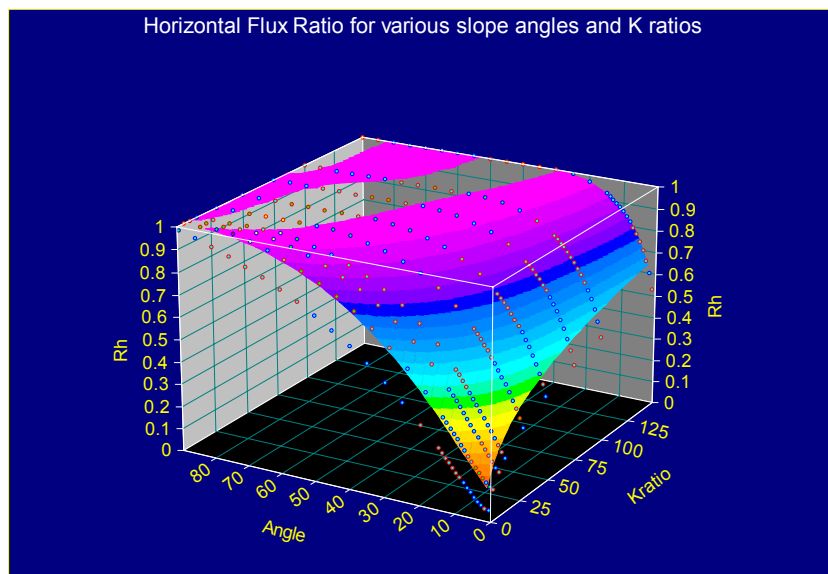


Figure 7: 3-Dimensional R_h envelope

5. ACKNOWLEDGEMENTS

This work was partially funded by the NSW State Salinity Strategy. The authors acknowledge useful discussions with Freeman Cook, Narendra Tuteja, and Aleksandra Rancic.

6. REFERENCES

- Chapman, T.G., and Dressler, R.F. (1984). Unsteady shallow groundwater flow over a curved impermeable boundary. *Water Resources Research*, 20(10): 1427-1434.
- Simunek, J., M. Sejna, and M. Th. van Genuchten, The HYDRUS-2D software package for simulating two-dimensional movement of water, heat, and multiple solutes in variably saturated media. Version 2.0, IGWMC - TPS - 53, Colorado School of Mines, Golden, Colorado, 251pp., 1999.
- Stauffacher, M., Bond, W., Bradford, A., Coram, J., Cresswell, H., Dawes, W., Gilfedder, M., Huth, N., Keating, B., Moore, A., Paydar, Z., Probert, M., Simpson, R., Stefanski, A., Walker, G. (2000). Assessment of Salinity Management Options for Wanilla, Eyre Peninsula: Groundwater and Crop Balance Modelling. CSIRO Tech Rep. 01/2000.
- Wooding, R.A. (1984). Groundwater flow over a sloping impermeable layer. 2. Exact solutions by conformal mapping. *Journal of Geophysical Research*, 71 (12): 2903-2910.